

# Endocytosis-dependent coordination of multiple actin regulators is required for wound healing

Yutaka Matsubashi, Camilla Coulson-Gilmer, and Tom H. Millard

Vol. 210 No. 3, August 3, 2015. Pages 419–433.

In Figures 1–4, arrows and arrowheads were inadvertently misplaced during the production process. Below are the corrected versions of the figures.

The HTML and PDF versions of this article have been corrected. The error remains only in the print version.

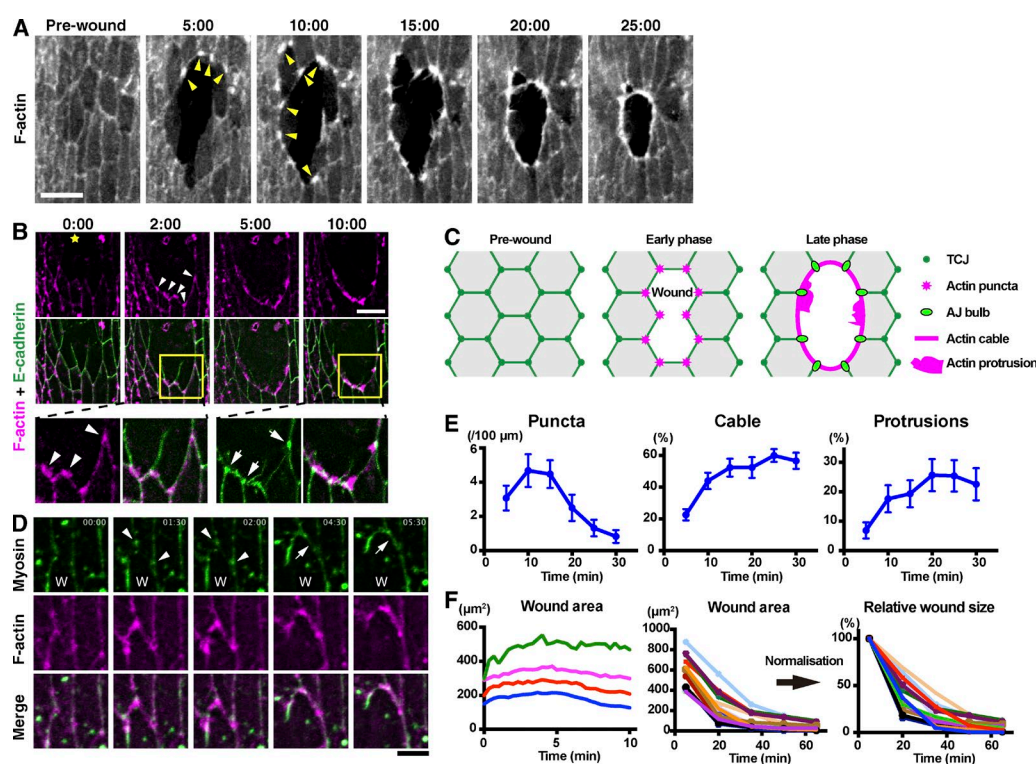


**Figure 1. Dynamics of F-actin, E-cadherin, and Myosin at wound edges.** (A) Time course of wound closure in *Drosophila* embryo expressing GFP-Moesin in the epidermis. Arrowheads indicate representative wound edge actin puncta. (B) The epidermis of a *Drosophila* embryo expressing the F-actin probe mCherry-Moesin (magenta) and E-cadherin-GFP (green) was wounded at the position marked by a yellow star and subjected to time-lapse live imaging. Bottom images show enlarged and enhanced images of the areas indicated by yellow squares in middle images. Arrowheads indicate actin puncta appearing at former-TCJs. Arrows indicate pronounced accumulations of E-cadherin where neighboring cells abut one another at the wound edge. (C) Cartoon illustrating the relationship between actin assembly and cell-cell junctions during wound healing. (D) Wound healing in an embryo expressing GFP-Zipper and mCherry-Moesin. W indicates position of wound. Arrowheads indicate myosin accumulations appearing and then enlarging at former-TCJs along the wound edge. Arrows indicate the formation of a link between two neighboring myosin accumulations. See also Video 1. (E) Wound closure was live imaged in embryos expressing GFP-Moesin and the prevalence of actin puncta, cable, and protrusions throughout the process was quantified as described in Materials and methods (graphs show means  $\pm$  SEM;  $n = 10$ –15 embryos). (F) GFP-Moesin-expressing embryos were wounded, and wound area throughout closure was measured. (left) Wound area in first 10 min after wounding plotted against time at 20-s intervals. Data from four individual embryos are shown. The wounds expanded until  $\sim 5$  min and then began to reduce in area. (middle) Wound area throughout closure for 15 individual wounds of varying size measured at 15-min intervals until 65 min after wounding. Note that the wounds all close over a broadly consistent time course and with similar dynamics. (right) Data in middle graph were normalized against the area at 5 min. Time points indicate time after wounding (minutes and seconds) in A, B, and D. Bars: (A and B) 10  $\mu\text{m}$ ; (D) 5  $\mu\text{m}$ .

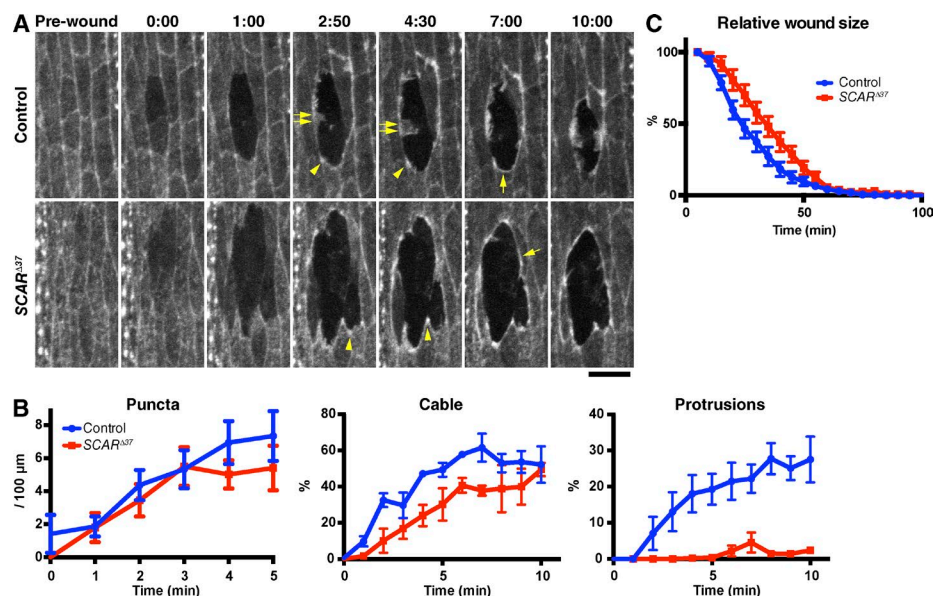


**Figure 2. SCAR function in actin remodeling at wound edges.** (A) Control and SCAR<sup>Δ37</sup> zygotic mutant embryos expressing GFP-Moesin were wounded and subjected to time-lapse imaging. Time points after wounding (minutes and seconds) are indicated. Note that although the actin puncta (arrowheads) and cable (single arrows) appear in both the control and mutant embryos, the formation of actin protrusions (double arrows) is severely reduced in the mutant, making its wound circumference markedly smoother than that of control. See also Video 2. Bar, 10 μm. (B) Quantitation of wound edge actin puncta, cable, and protrusion levels in control and zygotic SCAR<sup>Δ37</sup> embryos in the early phase of wound closure. *n* = 7–9 embryos. (C) Quantitation of wound closure in control and SCAR<sup>Δ37</sup> zygotic mutant embryos. Wound areas were normalized to the value at 5 min after wounding and plotted against time, as in Fig. 1 F. *n* = 4–17 embryos. Graphs show means ± SEM of the data.

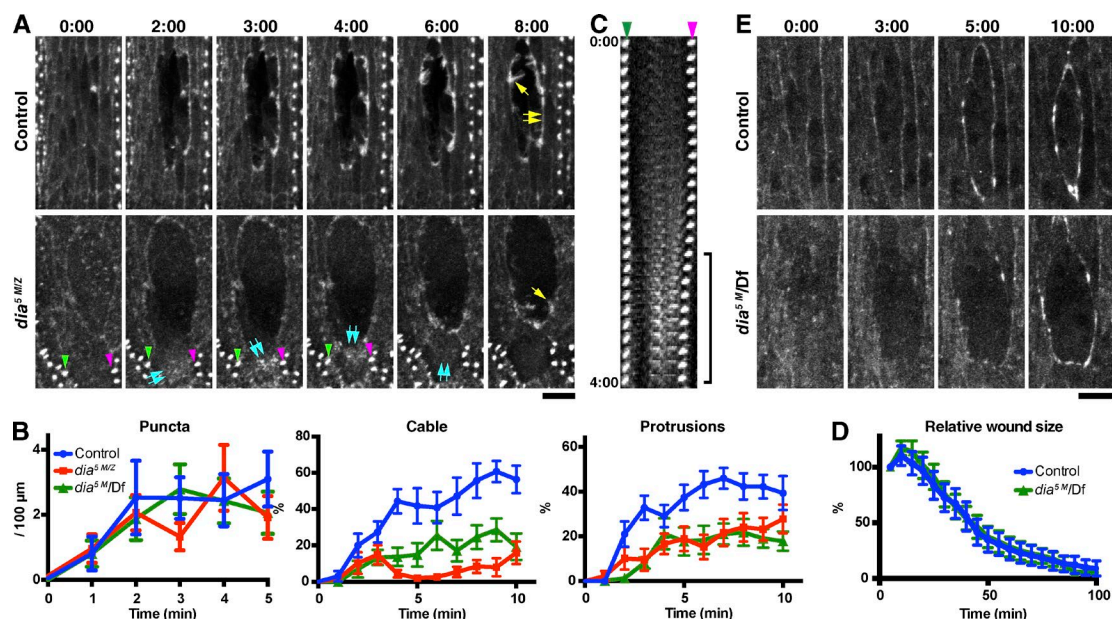


**Figure 3. Dia function in actin remodeling at wound edges.** (A) Time-lapse imaging of GFP-Moesin expressed in a control or *dia<sup>5</sup> M/Z* embryo. Yellow single arrows indicate actin protrusions; yellow double arrows indicate actin cable. Blue double arrows in the *dia<sup>5</sup> M/Z* images indicate diffuse assemblies of F-actin within a wound edge cell, which appear at 2 min, move upwards in the cell until 4 min and disappear by 6 min. See also Video 3. The dendrites indicated by the green and magenta arrowheads in the *dia<sup>5</sup> M/Z* images are visible in the kymograph in C. (B) Quantitation of wound edge actin puncta, cable, and protrusion levels in control, *dia<sup>5</sup> M/Z*, and *dia<sup>5</sup> M/Df* embryos in the early phase of wound closure. *n* = 9–13 embryos. (C) Kymograph analysis of the correlation between the formation of diffuse F-actin assemblies and cell contraction. The two dendrites indicated by the green and magenta arrowheads in this panel and in A are equivalent. Note that the distance between the two dendrites decreases when assemblies of F-actin (equivalent to blue double arrows in A) appear between them (bracket), consistent with this F-actin causing cell contraction. Images taken every 10 s until 4 min after wounding are shown. (D) Quantitation of wound closure in control and *dia<sup>5</sup> M/Df* embryos. Wound areas were normalized to the value at 5 min after wounding and plotted against time. *n* = 3–13 embryos. (E) Time-lapse imaging of GFP-Spaghetti-squash expressed in a control (+/Df) or *dia<sup>5</sup> M/Df* embryo. Time points indicate time after wounding (minutes and seconds). Graphs show means ± SEM of the data. Bars, 10 μm.

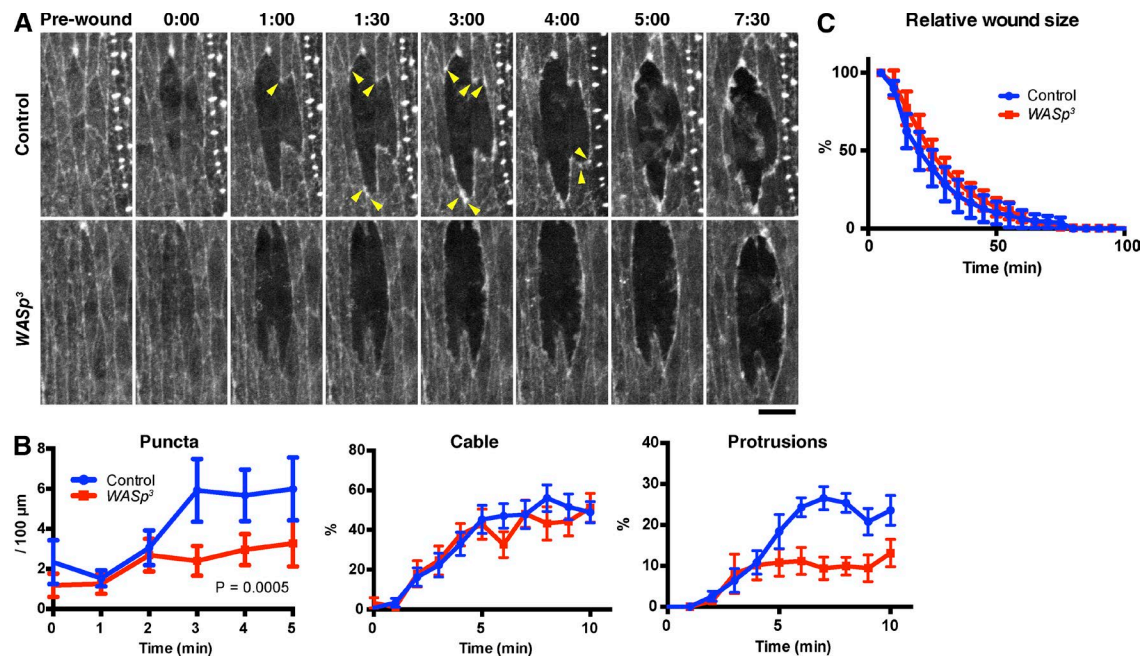


Figure 4. **WASP function in actin remodeling at wound edges.** (A) Time-lapse imaging of GFP-Moesin expressed in a control or *was<sup>3</sup>* zygotic mutant embryo. Arrowheads indicate actin puncta. Time points indicate time after wounding (minutes and seconds). Bar, 10  $\mu\text{m}$ . (B) Quantitation of wound edge actin puncta (left), cable (middle), and protrusions (right).  $n = 7-11$  embryos. (C) Quantification of wound closure. Wound areas were normalized against the value at 5 min after wounding and plotted against time.  $n = 6-8$  embryos. Graph show means  $\pm$  SEM of the data.